

Observation of exchange Coulomb interactions in the quantum Hall state at $\nu = 3$ A. B. Van'kov,^{1,2,*} T. D. Rhone,² A. Pinczuk,^{2,3} I. V. Kukushkin,¹ Loren N. Pfeiffer,⁴ Ken W. West,^{4,†} and V. Umansky⁵¹*Institute of Solid State Physics, RAS, Chernogolovka 142432, Russia*²*Department of Physics, Columbia University, New York, New York 10027, USA*³*Department of Applied Physics and Applied Mathematics, Columbia University, New York, New York 10027, USA*⁴*Bell Laboratories, Alcatel-Lucent, Murray Hill, New Jersey 07974, USA*⁵*Braun Center for Submicron Research, Weizman Institute of Science, 76100 Rehovot, Israel*

(Received 9 November 2010; revised manuscript received 11 May 2011; published 30 June 2011)

Coulomb exchange interactions of electrons in the $\nu = 3$ quantum Hall state are determined from two inter-Landau-level spin-flip excitations measured by resonant inelastic light scattering. The two coupled collective excitations are linked to inter-Landau-level spin-flip transitions arising from the $N = 0$ and $N = 1$ Landau levels. The strong repulsion between the two spin-flip modes in the long-wavelength limit is clearly manifested in spectra displaying Coulomb exchange contributions that are comparable to the exchange energy for the quantum Hall state at $\nu = 1$. Theoretical calculations within the Hartree-Fock approximation are in a good agreement with measured energies of spin-flip collective excitations.

DOI: [10.1103/PhysRevB.83.245325](https://doi.org/10.1103/PhysRevB.83.245325)

PACS number(s): 73.43.Lp, 71.70.Ej, 75.30.Ds

I. INTRODUCTION

The exchange Coulomb interaction energy of electrons plays key roles in quantum Hall systems, particularly at odd filling factors, $\nu = nhc/eB$ (n is the areal density), where the two-dimensional (2D) electron system evolves into a quantum Hall ferromagnet. This extends to fractional quantum Hall states, such as $\nu = 1/3$. One way to probe the exchange interaction is by measuring the energy of collective spin-flip (SF) excitations. The simplest one is the spin wave (SW), in which the Landau orbital quantization number does not change. At odd filling factors, the SW in the large-wave-vector limit is predicted to have a large exchange contribution, resulting in an enhanced spin gap.^{1,2} However, the actual energy values measured in activated transport experiments turned out to be significantly below theoretical estimates. These discrepancies occur in both the integer and the fractional quantum Hall regimes. Possible reasons for the differences may be due to the impact of spin textures (skyrmions)⁴⁻⁶ and of weak residual disorder.⁷⁻⁹

Nevertheless, there exist venues for experimental access to Coulomb exchange interactions which yield results in close agreement with theoretical predictions. This is accomplished by studying the excitations of collective modes with spin degrees of freedom using inelastic light scattering. At odd integer filling factors the long-wavelength SW is a minimum-energy collective excitation. The long-wavelength SW mode approaches the bare Zeeman energy^{1,2,10} and carries marginal information about electron-electron interactions. However, inelastic light scattering methods enable the direct determination of exchange Coulomb interactions from measurements of SF collective excitations across cyclotron gaps.¹¹⁻¹⁴ In these SF excitations, there is simultaneous change in the Landau quantization number and orientation of spin. Long-wavelength SF excitations represent probes that are almost insensitive to perturbations on length scales exceeding the characteristic size of the quasiparticle-quasihole pair magnetoexciton, which is of the order of the magnetic length, $l_o = (\hbar c/eB)^{1/2}$, where B is the perpendicular component of the magnetic field.

At $\nu = 1$ the electron-electron interaction affects the energy of the long-wavelength cyclotron SF mode, which involves a change of the Landau quantization number by $+1$. This mode is shifted upward from the cyclotron energy by about half the full exchange energy in the large-wave-vector SW. Studies of the cyclotron SF mode at $\nu = 1$ have shown that the Coulomb exchange contribution to its energy scales as \sqrt{B} and that its value is softened by the spread of the electron wave function in the direction normal to the 2D plane. Theoretical predictions are in good agreement with measured mode energies determined as a function of electron concentration and quantum well width.^{11,12}

We report inelastic light scattering measurements of collective inter-Landau-level (LL) excitations in the quantum Hall state around $\nu = 3$. All collective excitations are identified in inelastic light scattering spectra, and their energies compared with theoretical calculations. We identified two coupled cyclotron SF modes arising from the $N = 0$ and $N = 1$ LLs and interpreted the results in terms of Coulomb exchange interactions. We determined that the coupled cyclotron SF modes at $\nu = 3$ are subject to large Coulomb exchange interactions that are comparable to the exchange energy associated with the quantum Hall state at $\nu = 1$.

There is great current interest in the role of the spin degree of freedom in the remarkable quantum Hall phases in the $N = 1$ LL.¹⁵⁻¹⁷ We find that exchange Coulomb interactions in the $N = 1$ LL are comparable to those in the $N = 0$ LL. This observation suggests that the exotic collective states that emerge in the partially populated $N = 1$ level are linked to the differences in correlation effects between the two levels. Moreover, studies at $\nu = 3$ will set the foundation for future investigation of fractional quantum Hall states of the $N = 1$ LL, such as $\nu = 7/3$, $8/3$, and $5/2$.

II. COLLECTIVE EXCITATIONS IN THE $\nu = 3$ QUANTUM HALL FERROMAGNET

Figure 1(a) shows the schematic representation of five lowest-energy collective excitations in the case of filling factor

$\nu = 3$: one intra-LL and four excitations across the cyclotron gap. They are shown as magnetoexcitons consisting of an electron promoted from a filled LL and bound to an effective hole left in the “initial” LL. This representation is exact in the limit of a strong magnetic field where the parameter $r_c = E_c/\hbar\omega_c$ is small.^{1–3} E_c is the Coulomb energy and $\hbar\omega_c$ is the cyclotron energy. The set of dispersion curves of the collective modes can be described in the following way:²

$$E_{m,\delta S_z}(k) = m\hbar\omega_c + g\mu_B B\delta S_z + \Delta E_{m,\delta S_z}(k), \quad (1)$$

where m is the change in the LL index and $g\mu_B B\delta S_z$ is the bare Zeeman energy associated with the SF mode. The last term, $\Delta E_{m,\delta S_z}(k)$, is responsible for the dispersion and comprises contributions from the many-body Coulomb interaction and exchange energies in the initial and the excited states. We focus on the excitation spectra with $m = 0$ and $m = 1$.

At $\nu = 3$ the four inter-LL transitions with $m = 1$ shown in Fig. 1(a) are not independent. They couple via the Coulomb interaction to yield two pairs of excitations. The two inter-LL excitations with no change in the spin degree of freedom ($\delta S_z = 0$) are the in-phase magnetoplasmon (MP) mode and the antiphase plasmon (AP) mode. The two excitations (coupled modes) with change in the spin degree of freedom ($\delta S_z = -1$) are the cyclotron spin-flip (SF) excitations SF1 and SF2.

In first-order perturbation theory the dispersion curves of the coupled modes are expressed as follows:

$$E_{1,2}(k) = \frac{\mathcal{E}_1(k) + \mathcal{E}_2(k)}{2} \pm \sqrt{\left(\frac{\mathcal{E}_1(k) - \mathcal{E}_2(k)}{2}\right)^2 + \Delta_{12}(k)^2}, \quad (2)$$

where $\mathcal{E}_{1,2}(k)$ are the energies of single transitions either with or without SF, and $\Delta_{12}(k)$ is responsible for coupling. For MP and AP excitations, this theory yields a vanishing Coulomb term $\Delta E(k)$ in the long-wavelength limit. Unlike the MP mode, for which Kohn’s theorem¹⁸ is valid, the experimental values of the energy of the AP mode are red-shifted relative to the cyclotron energy at integer filling factors $\nu \geq 2$. The experimental results have been reported in Refs. 19,20 and 23 and the explanation was given in the framework of second-order perturbation theory.^{21,23}

We calculated the dispersion of SF1 and SF2 at $\nu = 3$ in terms of matrix elements $\tilde{V}_{\alpha\beta\gamma\delta}^{(1)}(k)$ introduced in Ref. 2:

$$\begin{aligned} \mathcal{E}_1(k) &= \hbar\omega_c + |g\mu_B B| + \Sigma_{0\uparrow,1\downarrow} - \tilde{V}_{1001}^{(1)}(k), \\ \mathcal{E}_2(k) &= \hbar\omega_c + |g\mu_B B| + \Sigma_{1\uparrow,2\downarrow} - \tilde{V}_{2112}^{(1)}(k), \\ \Delta_{12}(k) &= \tilde{V}_{1102}^{(1)}(k), \end{aligned} \quad (3)$$

where $\Sigma_{0\uparrow,1\downarrow} = \tilde{V}_{0000}^{(1)}(0) + \tilde{V}_{0101}^{(1)}(0) - \tilde{V}_{1010}^{(1)}(0)$ and $\Sigma_{1\uparrow,2\downarrow} = \tilde{V}_{1010}^{(1)}(0) + \tilde{V}_{1111}^{(1)}(0) - \tilde{V}_{2020}^{(1)}(0)$ are the differences in exchange self-energies between the excited and the ground states for the two single SF transitions between adjacent LLs depicted in Fig. 1(a). The calculated dispersion curves for all four inter-LL excitations with $B_{\perp} = 5.3$ T are plotted with solid lines in Fig. 1(b). For comparison with experiment, we took into account the finite thickness of the 2D-electron system. To do this, the Fourier component of the effective e - e interaction

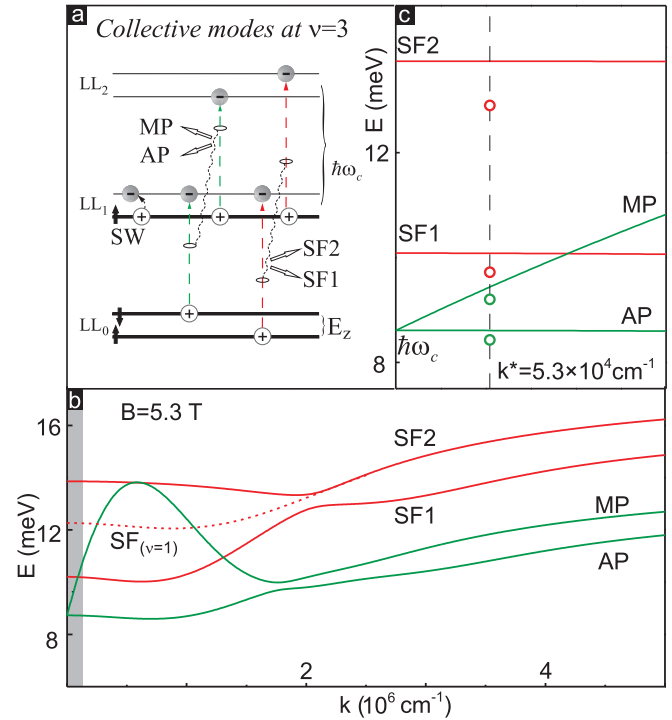


FIG. 1. (Color online) (a) Schematic representation of the formation of collective modes at $\nu = 3$ from single-electron transitions. The spin wave (SW) is described as a single spin-flip transition within half-filled LL₁. MP and AP are formed as in-phase and antiphase combinations of two inter-LL transitions with $\delta S_z = 0$ (green). Cyclotron spin-flip modes SF1 and SF2 arise from analogous combinations of inter-LL transitions with $\delta S_z = -1$ (red). (b) Dispersion curves of inter-LL excitations calculated for $B_{\perp} = 5.3$ T within the first-order Hartree-Fock approximation are shown. Here the finite thickness of the 2D electron system (for sample A with a 24-nm quantum well) is taken into account via the geometric form factor. The dashed line represents the dispersion of the cyclotron spin-flip mode at $\nu = 1$ under the same magnetic field. (c) Zoomed-in image of the long-wavelength region in (b) shaded light gray. The dashed vertical line indicates the experimental in-plane momentum $k^* = 5.3 \times 10^4 \text{ cm}^{-1}$. Open circles represent experimental data.

potential $\vartheta(q) = 2\pi e^2/\epsilon q$ was multiplied by the geometric form factor $F(q)$, calculated via the self-consistent solution of the Poisson and Schrödinger equations.²²

Both cyclotron SF modes at $\nu = 3$ are significantly blue-shifted from the cyclotron energy and are nearly dispersionless in the long-wavelength limit [see Figs. 1(b) and 1(c)]. Furthermore, they strongly repel each other, especially at small momenta. As a result, the Coulomb energy of SF2 in the long-wavelength limit is even higher than that of the analogous inter-LL SF mode in the fully spin-polarized quantum Hall state at $\nu = 1$.^{11,12} On the contrary, the energy of SF1 is reduced. The Coulomb energy of the long-wavelength mode SF2 is just 15% lower than the energy of the SW at $k \rightarrow \infty$ (shown in the bottom inset in Fig. 2)—the electron exchange energy in LL₁. One of the intriguing results of this calculation is that the highest energy spin-flip excitation, SF2, corresponds to the antiphased combination of two single electron transitions, while SF1 corresponds to the in-phase

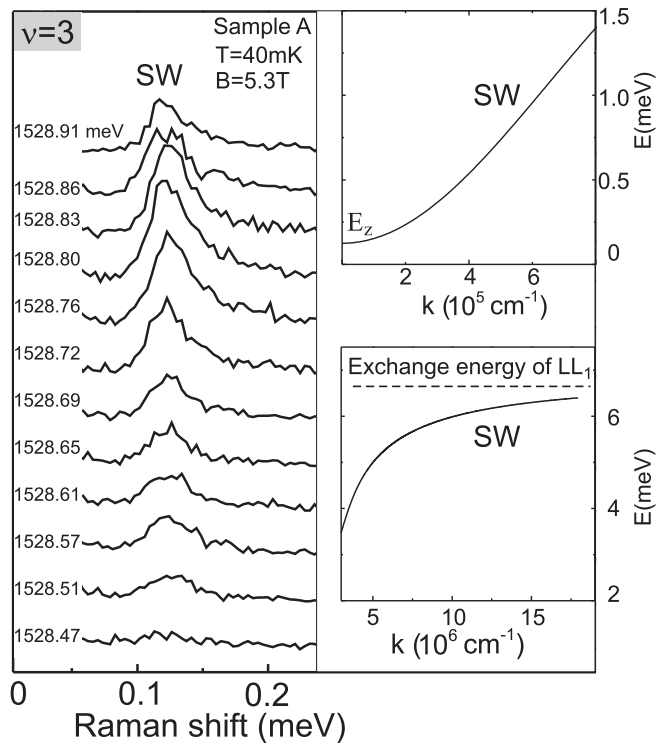


FIG. 2. Inelastic light scattering spectra of the intra-LL SW mode at $\nu = 3$ and $B = 5.3$ T taken at different laser photon energies (shown at the left). Insets: SW dispersion curves calculated within the Hartree-Fock approximation² for a 24-nm-wide quantum well. The top inset shows the long-wave part and the bottom one displays the short-wave part of the SW dispersion. At the experimental in-plane momentum the energy of the SW is indistinguishable from E_z .

combination. The situation is reversed in the case of the $\delta S_z = 0$ modes - MP (inphase) and AP (antiphase). As shown in the case of the AP mode,^{20,21} the first-order perturbation theory overestimates the energy in the long-wavelength limit. Although second-order corrections are exactly computed only for AP at $k = 0$, they are likely to be of the same order for SF1 and SF2.

III. EXPERIMENTAL TECHNIQUE

Inelastic light scattering measurements were performed on three high-quality GaAs/Al_{0.3}Ga_{0.7}As heterostructures. Sample A was a 24-nm-wide single quantum well (SQW) with $n_e = 3.85 \times 10^{11} \text{ cm}^{-2}$ and low-temperature mobility $\mu \gtrsim 17 \times 10^6 \text{ cm}^2/\text{V} \cdot \text{s}$. The other two GaAs/Al_{0.3}Ga_{0.7}As heterostructures used had the following parameters: sample B was a 16-nm SQW, with $n_e = 2.9 \times 10^{11} \text{ cm}^{-2}$ and $\mu \gtrsim 3 \times 10^6 \text{ cm}^2/\text{V} \cdot \text{s}$; and sample C was a 30-nm SQW, with $n_e = 2.47 \times 10^{11} \text{ cm}^{-2}$ and $\mu \gtrsim 30 \times 10^6 \text{ cm}^2/\text{V} \cdot \text{s}$. Optical experiments were performed in a ³He/⁴He dilution refrigerator with windows for optical access. The sample temperature varied from $T = 40$ mK to 1.7 K. The backscattering geometry was used with the sample tilted at an angle $\theta = 20^\circ$ to the normal of the sample surface. The perpendicular component of the magnetic field is $B = B_T \cos \theta$, where B_T is the total magnetic field. Resonant inelastic light scattering spectra were

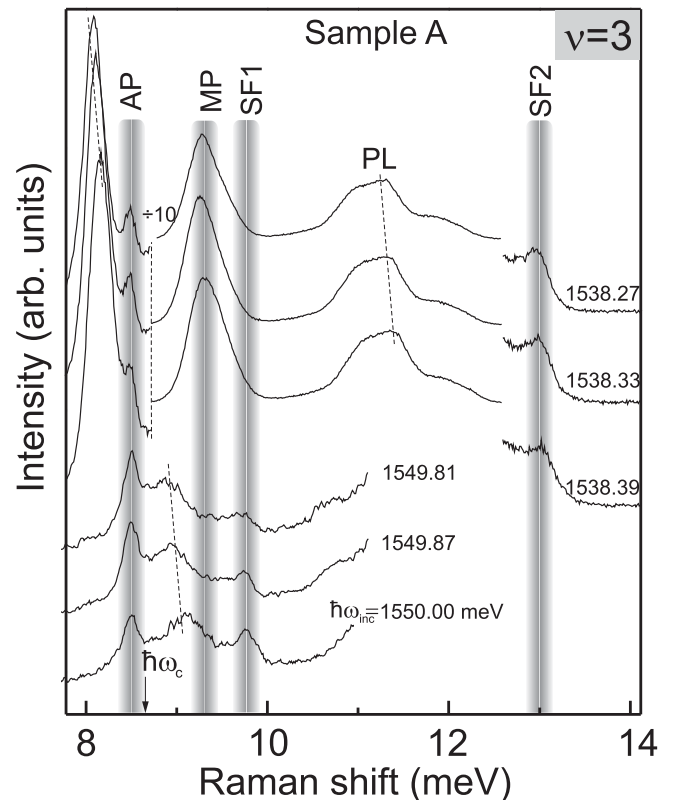


FIG. 3. Inelastic light scattering spectra of inter-LL excitations at $\nu = 3$ and $B_\perp = 5.3$ T taken at different incident photon energies (indicated on the right side of the spectra). The upper three spectra correspond to the resonant incident photon energies when electrons were promoted from the valence band to the second Landau level. Lower spectra were taken under resonant conditions when electrons were excited to the third Landau level. Gray vertical columns mark inelastic light scattering lines. The rest of the spectrum is composed of the luminescence bands, marked by slanted dashed lines. Note: The weak spectral feature between AP and SF1 in the lower spectra is a photoluminescence line since its spectral position changes upon variation of the laser photon energy.

obtained by tuning the incident photon energy of a Ti:sapphire laser close to the fundamental optical gap of GaAs to enhance the light scattering cross section. The power density was kept below $10^{-4} \text{ W}/\text{cm}^2$ for measurements at temperatures around 40 mK. The in-plane momentum transferred to the excitations in the experimental geometry was about $5.3 \times 10^4 \text{ cm}^{-1}$. The scattered signal was dispersed by a T-64000 triple-grating spectrometer working in additive and subtractive modes. Spectra were acquired by optical multichannel detection. The combined resolution of the system was about 0.02 meV. Spectral weight from inelastic light scattering and luminescence may be distinguished in the following manner: on an absolute energy scale, inelastic light scattering lines are seen to shift when tuning the incident photon energy. Spectral weight from luminescence, however, does not change spectral position. The reverse is true on an energy shift (Raman shift) scale: inelastic light scattering lines were stationary, while luminescence lines moved with changing incident photon energy.

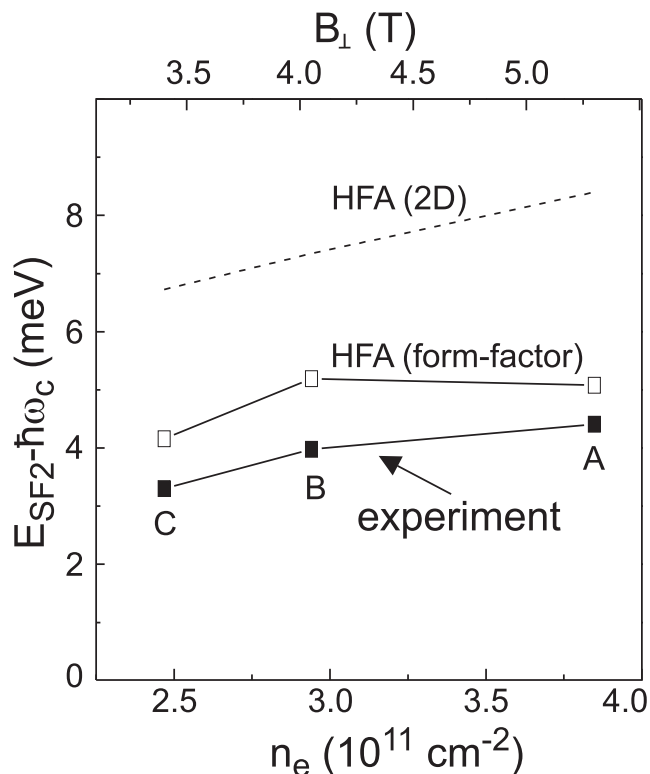


FIG. 4. Energy shift of SF2 from $\hbar\omega_c$ measured in three samples with different 2D-electron densities and quantum well widths. Filled symbols depict experimental values for samples A, B, and C. Open symbols are Hartree-Fock approximation calculation results obtained using the geometrical form factor for the quantum well size of each sample. The dashed curve corresponds to the Hartree-Fock approximation results calculated for the ideal 2D-electron system.

IV. EXPERIMENTAL RESULTS AND DISCUSSION

The resonant enhancement of the intensities of light scattering spectra of the SW at $\nu = 3$ for sample A is displayed in Fig. 2. This intra-LL excitation has $m = 0$ (no change in LL index). The SW is at the bare Zeeman energy with g factor $|g| = 0.37$, the value of which is affected by conduction band nonparabolicity effects.¹⁰ The SW energy corresponds to the leftmost part of the dispersion shown in the top inset in Fig. 2. Very small changes in the laser photon energy (~ 0.5 meV) dramatically affect the line intensity, indicating the importance of resonance enhancement. The strong SW shown in Fig. 2 is consistent with the ferromagnetic character of the quantum Hall state at $\nu = 3$.

Similar resonance enhancement conditions exist for observation of the inter-LL excitations reported below. Figure 3 displays a sequence of typical spectra measured on sample A at several laser photon energies. Inelastic light scattering lines from all four inter-LL excitations are present in the spectra. The upper three spectra were taken under resonant conditions such that incident photons excite electrons from the valence band to the states in LL_2 .

Under these conditions, Raman lines from AP, MP and SF2 are all observed. In these spectra the MP line overlaps the luminescence band, which causes an additional resonant

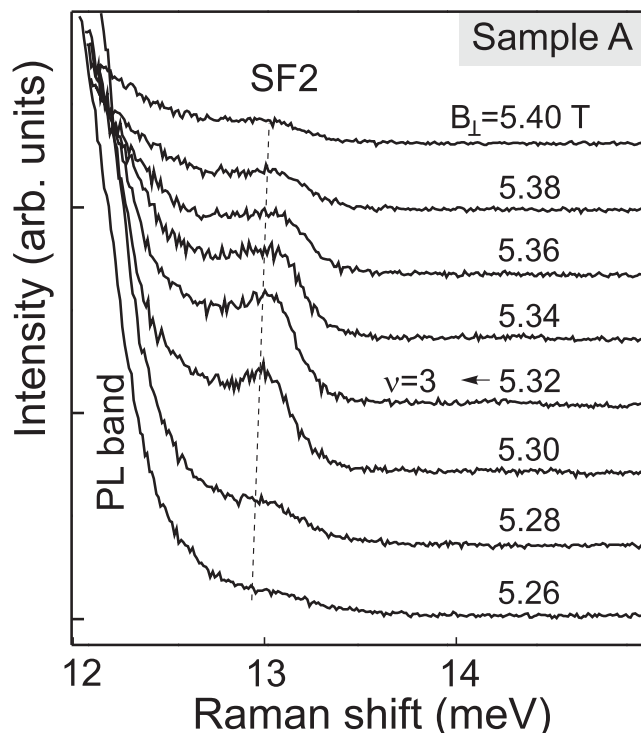


FIG. 5. Magnetic field evolution of the inelastic light scattering spectrum of SF2 in the vicinity of $\nu = 3$, taken at the fixed incident photon energy $\hbar\omega_{inc} = 1538.33$ meV. At $|\Delta B_{\perp}| \sim 0.15$ T, the line nearly vanishes from the spectrum. The strong line in the left part of the spectrum originates from photoluminescence.

enhancement. Consequently, the MP line is strongly enhanced in intensity and somewhat broadened compared to the other Raman lines. The lower three spectra are measured under other resonant conditions: electrons are promoted from the valence band to LL_3 . In this case, AP and SF1 Raman lines are observed. The nature of the resonance conditions of inelastic light scattering for the inter-LL collective modes possibly lies in the complex mixing of single-electron transitions constituting the collective modes and the ability of the incident photons to excite them to the appropriate LLs.

The magnetoplasmon (MP) and antiphased plasmon are seen to be shifted from the cyclotron energy (depicted by the arrow in Fig. 3) by 0.61 and -0.19 meV, respectively. The blue shift of the MP results from the 2D-plasma energy at the nonzero in-plane momentum used in the experiment. In fact, the MP is the only dispersive mode in the range of experimentally accessible momenta [see Fig.1(c)]. The energy of AP is below $\hbar\omega_c$ by 0.19 meV. The theory developed in Ref. 23 gives $\Delta E_{AP}(0) \approx -0.25$ meV for this magnetic field and quantum well width.

In the case of the two cyclotron spin-flip modes SF1 and SF2, which are blue-shifted from $\hbar\omega_c$, we compare the experimental energy shifts with those calculated theoretically [within the first-order Hartree-Fock approximation, taking into account the quantum well width; see Fig. 1(c)]. The shift of SF2 energy from $\hbar\omega_c$ for all three samples is plotted in Fig. 4 (filled symbols). The results of the Hartree-Fock approximation calculation are shown in the same plot for

comparison. The experimental and theoretical values agree quite well, provided the actual width of the quantum well is taken into account via the geometrical form factor (open symbols in the plot), whereas the theoretical curve for an ideal 2D electron system overestimates the energies. The plotted electron-density dependence of the SF2 energy shift is not quite monotonic since different points correspond to different quantum well widths.

We also find a marked dependence on magnetic field in which SF1 and SF2 modes are observed only in the narrow interval $\Delta B_{\perp} \simeq 0.15$ T around $\nu = 3$ (see Fig. 5). Outside this field range, the lines disappear from the spectrum. We conclude that the stability of SF excitations is inherent in the ferromagnetic state $\nu = 3$. The Coulomb energy of SF2 is close to the estimated full exchange energy of electrons in LL_1 . The latter is represented by the energy limit of the short-wavelength SW at $\nu = 3$ (see the bottom inset in Fig. 2). This asymptotic value is about three-fourths of the analogous quantity in the fully spin-polarized state $\nu = 1$.

In summary, we have observed and identified four inter-LL collective excitations and an intra-LL spin-wave at $\nu = 3$, using inelastic light scattering. Among these excitations are

two cyclotron SF modes, which interact repulsively in the long-wavelength limit. As a result, the more energetic SF2 acquires a huge exchange contribution to the energy, in close agreement with the theoretically estimated exchange energy of electrons in the first LL. The experimentally measured energies of all excitations are in good agreement with the Hartree-Fock calculations, corrected for the finite thickness of the 2D-electron system.

ACKNOWLEDGMENTS

The authors acknowledge support from the US Civilian Research and Development Foundation and the Russian Foundation for Basic Research. T.D.R. and A.P. were supported by the National Science Foundation under Grant Nos. DMR-0352738 and DMR-0803445 and by the Nanoscale Science and Engineering Initiative of the National Science Foundation under Award Nos. CHE-0117752 and CHE-0641523. T.D.R. and A.P. were also supported by the Department of Energy under Grant No. DE-AIO2-04ER46133 and by a research grant from the W. M. Keck Foundation.

*Corresponding author: vasash@mail.ru

[†]Present address: Department of Electrical Engineering, Princeton University, Princeton, New Jersey 08544, USA

¹Yu. A. Bychkov, S. V. Iordanskii, and G. M. Eliashberg, *JETP Lett.* **33**(3), 143–146 (1981).

²C. Kallin and B. I. Halperin, *Phys. Rev. B* **30**, 5655 (1984).

³Yu. A. Bychkov and E. I. Rashba, *Sov. Phys. JETP* **58**, 1062–1073 (1983).

⁴A. Schmeller, J. P. Eisenstein, L. N. Pfeiffer, and K. W. West, *Phys. Rev. Lett.* **75**, 4290 (1995).

⁵A. F. Dethlefsen, R. J. Haug, K. Vyborny, O. Certik, and A. Wojs, *Phys. Rev. B* **74**, 195324 (2006).

⁶J. G. Groshaus, I. Dujovne, Y. Gallais, C. F. Hirjibehedin, A. Pinczuk, Y.-W. Tan, H. Stormer, B. S. Dennis, L. N. Pfeiffer, and K. W. West, *Phys. Rev. Lett.* **100**, 046804 (2008).

⁷A. Usher, R. J. Nicholas, J. J. Harris, and C. T. Foxon, *Phys. Rev. B* **41**, 1129 (1990).

⁸V. T. Dolgoplov, A. A. Shashkin, A. V. Aristov, D. Schmerek, W. Hansen, J. P. Kotthaus, and M. Holland, *Phys. Rev. Lett.* **79**, 729 (1997).

⁹V. S. Khrapai, A. A. Shashkin, E. L. Shangina, V. Pellegrini, F. Beltram, G. Biasiol, and L. Sorba, *Phys. Rev. B* **72**, 035344 (2005).

¹⁰M. Dobers, K. von Klitzing, and G. Weimann, *Phys. Rev. B* **38**, 5453 (1988).

¹¹A. Pinczuk, B. S. Dennis, D. Heiman, C. Kallin, L. Brey, C. Tejedor, S. Schmitt-Rink, L. N. Pfeiffer, and K. W. West, *Phys. Rev. Lett.* **68**, 3623 (1992).

¹²A. B. Van'kov, L. V. Kulik, I. V. Kukushkin, V. E. Kirpichev, S. Dickmann, V. M. Zhilin, J. H. Smet, K. von Klitzing, and W. Wegscheider, *Phys. Rev. Lett.* **97**, 246801 (2006).

¹³A. S. Zhuravlev, A. B. Van'kov, L. V. Kulik, I. V. Kukushkin, V. E. Kirpichev, J. H. Smet, K. von Klitzing, V. Umansky, and W. Wegscheider, *Phys. Rev. B* **77**, 155404 (2008).

¹⁴A. B. Van'kov, L. V. Kulik, S. Dickmann, I. V. Kukushkin, V. E. Kirpichev, W. Dietsche, and S. Schmult, *Phys. Rev. Lett.* **102**, 206802 (2009).

¹⁵G. A. Csathy, J. S. Xia, C. L. Vicente, E. D. Adams, N. S. Sullivan, H. L. Stormer, D. C. Tsui, L. N. Pfeiffer, and K. W. West, *Phys. Rev. Lett.* **94**, 146801 (2005).

¹⁶C. R. Dean, B. A. Piot, P. Hayden, S. Das Sarma, G. Gervais, L. N. Pfeiffer, and K. W. West, *Phys. Rev. Lett.* **101**, 186806 (2008).

¹⁷T. D. Rhone, J. Yan, Y. Gallais, A. Pinczuk, L. N. Pfeiffer, and K. W. West, *Phys. Rev. Lett.* **106**, 196805 (2011).

¹⁸W. Kohn, *Phys. Rev.* **123**, 1242 (1961).

¹⁹M. A. Eriksson, A. Pinczuk, B. S. Dennis, S. H. Simon, L. N. Pfeiffer, and K. W. West, *Phys. Rev. Lett.* **82**, 2163 (1999).

²⁰L. V. Kulik, I. V. Kukushkin, S. Dickmann, V. E. Kirpichev, A. B. Van'kov, A. L. Parakhonsky, J. H. Smet, K. von Klitzing, and W. Wegscheider, *Phys. Rev. B* **72**, 073304 (2005).

²¹S. Dickmann and I. V. Kukushkin, *Phys. Rev. B* **71**, 241310(R) (2005).

²²M. S.-C. Luo, S.L. Chuang, S. Schmitt-Rink, and A. Pinczuk, *Phys. Rev. B* **48**, 11086 (1993).

²³L. V. Kulik, S. Dickmann, I. K. Drozdov, A. S. Zhuravlev, V. E. Kirpichev, I. V. Kukushkin, S. Schmult, and W. Dietsche, *Phys. Rev. B* **79**, 121310(R) (2009).